Scientific Research Publishing

Materials Sciences and Applications, 2025, 16(5), 239-251
https://www.scirp.org/journal/msa
ISSN Online: 2153-1188
ISSN Print: 2153-117X

Optimization and Mechanism Study on Electrothermal Performance of Polypropylene/Antioxidant Composite Systems Based on Molecular Dynamics

Feng Bin[1], Jixiang Feng[1], Shaobo Liu[1*], Fangwei Liang[2], Zhensheng Tan[1], Denghui Jiang[1]

[1]School of Physics and Electronic Science, Changsha University of Science and Technology, Changsha, China
[2]Tsinghua University, State Key Laboratory of Power System Operation and Control, Beijing, China
Email: liushaobo@csust.edu.cn

How to cite this paper: Bin, F., Feng, J.X., Liu, S.B., Liang, F.W., Tan, Z.S. and Jiang, D.H. (2025) Optimization and Mechanism Study on Electrothermal Performance of Polypropylene/Antioxidant Composite Systems Based on Molecular Dynamics. *Materials Sciences and Applications*, **16**, 239-251.
https://doi.org/10.4236/msa.2025.165014

Received: March 30, 2025
Accepted: May 18, 2025
Published: May 21, 2025

Abstract

Polypropylene (PP) emerges as a promising power cable insulation material, with its electrothermal performance fundamentally determining application potential and operational durability. Meanwhile, antioxidants, renowned for their ability to enhancing thermal stability and insulating performance of polyolefins, offer a viable strategy for optimizing PP. Thus, this study establishes molecular dynamics models for PP/antioxidant systems with antioxidant type as a variable, to investigate the microstructural evolution and electrothermal properties of antioxidant-modified PP across different temperatures. The simulation results indicate that compared to PP neat system, PP/AO736 system shows a 26K increase in glass transition temperature, a 13.88% reduction in relative dielectric constant, and a 37.6% enhancement in breakdown strength at 400 K. Besides, PP/HP system demonstrates advantages in regulating heat transfer, with a 33.1% improvement in thermal conductivity at 300 K. These findings provide methodological guidance for improving the electrical and thermal properties of PP.

Keywords

Polypropylene, Molecular Dynamics, Antioxidant, Electrothermal Performance

1. Introduction

Polypropylene (PP), a polymer material with excellent electrical insulation performance, has been extensively utilized in power cables systems [1]. However, PP

exhibit susceptibility to oxidative degradation and limited thermal stability. Under high electric field or elevated-temperature conditions, substantial space charge accumulates within PP, triggering irreversible electrical treeing failure and consequently degrading the dependability of power cables. Notably, when the ambient temperature exceeds 380 K, the conductive loss of PP shows an exponential ascent, accompanied by a progressive decline in breakdown strength. This nonlinear deterioration characteristics cause a bottleneck issue that restricts the application of PP in ultra-high voltage direct current (DC) cables [2]. Therefore, the development of modified PP systems with synergistic electrical and thermal stability has become an important technological pathway for enhancing the reliability of power cables.

In recent years, scholars have carried out in-depth research on the modification of PP. Demirbas *et al.* achieved a tensile strength of 20.1 MPa by incorporating 2.5% SiO_2 into PP [3]. Guo *et al.* added a β-nucleating agent to PP, significantly enhancing its mechanical properties; the tensile strength and impact resistance were increased by 54% and 53%, respectively [4]. Li *et al.* introduced high dielectric barium strontium titanate (BST) into the PP matrix, observing that when the BST content reached 20%, the interfacial charge density of composite material decreased to 3.83×10^{-5} C/m^2 [5]. Yokoi *et al.* modified PP by grafting carboxylic acid, resulting in a 56% increase in tensile strength, although the tensile modulus decreased by 34% [6]. Chen *et al.* reported that the fracture energy of maleic anhydride-modified PP could reach up to 14.82 KJ/m^2 [7]. Lee *et al.* blended isotactic PP with a small amount of polyvinylidene fluoride via melt mixing, demonstrating that DC breakdown voltage of the modified material at 298 K and 383 K was 110% and 149% higher than that of PP neat, respectively [8]. Guo *et al.* filled PP with carbon nanotubes functionalized with eight functional groups, increasing the melting temperature of composite by 88.85 K [9]. Despite significant advancements in optimizing mechanical property or independently enhancing electrical or thermal properties, there is an obvious gap in research on synergistic electrothermal enhancement.

Molecular dynamics (MD) serves as a core technology for analyzing the property of polymer composites, effectively addressing the high-cost and time-consuming limitations inherent in conventional trial-and-error experimental approaches [10]. It is difficult to directly observe microstructural evolution within PP, whereas MD simulations, through dynamic tracking of atomic-scale, can not only reveal the intrinsic rules in governing the microscopic behavior of material, but also offer theoretical guidance for the design of high-performance composites.

Current investigations on the enhancement of electrical performance of PP insulation materials primarily focus on modification using inorganic nanoparticles. However, in practical engineering applications, inorganic nanofillers tend to induce agglomeration, thereby deteriorating the dielectric property of PP and significantly limiting their practical use in industrial settings. In contrast, organic small molecule additives exhibit great advantages in the modification of PP, due

to their excellent dispersion property and customizable functional groups [11]. Antioxidants have shown positive effect in enhancing the stability of polyolefin materials, such as polyethylene [12]. Nevertheless, there has been no report on the utilization of antioxidant to modify PP to achieve synergistic improvements in both electrical and thermal performance.

Therefore, in this paper, MD simulations are employed to construct PP composite systems, which incorporate three typical antioxidants, *i.e.*, 3,5-di-tert-butyl-4-hydroxyhydrocinnamate (AO1010), 4,4′-thiobis-2-methyl-6-tert-butylphenol (AO736), and 3,5-Di-tert-butyl-4-hydroxybenzaldehyde (HP). Specifically, four comparative models are established: PP neat, PP/AO1010, PP/AO736, and PP/HP. Besides, the performance parameters, including glass transition temperature (T_g), thermal conductivity (λ), relative dielectric constant (ε_r), and breakdown strength (E_b) of PP, are obtained. Furthermore, to understand the mechanisms underlying the performance changes, the free volume fraction is analyzed at the microscopic level.

2. Calculation Models and Methods

MD simulations are performed using the COMPASS forcefield, with temperature and pressure regulated via Nose-Hoover and Berendsen method, respectively. In the simulation, the system pressure and time step are set to 1×10^{-4} GPa and 1 fs, respectively; electrostatic and van der Waals interactions are calculated through Ewald summation and Atom-Based methods, respectively.

2.1. Modeling

This paper uses Materials Studio (MS) software to establish simulation models. The modeling process is illustrated in Figure 1, and the main steps are described as follows:

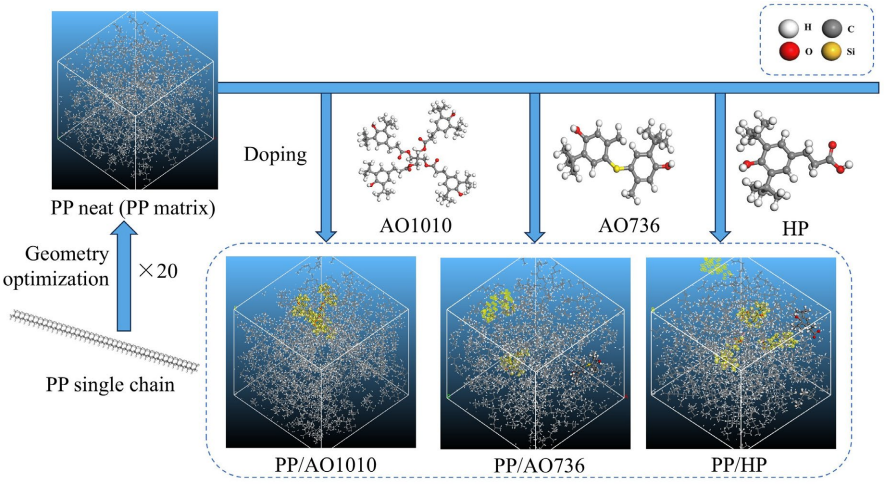

Figure 1. Modeling process.

(i) Constructing the molecular conformation of isotactic PP, AO1010, AO736,

and HP. To balance computational complexity and efficiency, the degree of polymerization for single PP chain is set to 40. Subsequently, the Geometry Optimization function in the Forcite module is employed to optimize their geometries. In this process, the energy convergence accuracy and maximum iteration are set to 2.0×10^{-5} kcal/mol and 5000, respectively, and the optimization algorithm choose Smart.

(ii) Determining the PP matrix conformation with the lowest energy. A three-dimensional amorphous structure consisting of 20 PP chains is designed using the Amorphous Cell (AC) module, and a total of 10 conformations are generated. Then, the Energy function in the Forcite module is used to calculate the energy of each conformation, and the one with the lowest energy is selected as the initial structure, whose density simulated is 0.83 g/cm^3, showing an error of only 6.74% when compared to the experimentally measured value of 0.89 g/cm^3 [13]. In this process, the initial density and temperature are set to 0.6 g/cm^3 and 300 K, respectively.

(iii) Constructing PP/antioxidant simulation models. The antioxidants are incorporated into the PP matrix via the Construction function in AC module. Consequently, four simulation models are established: PP neat, PP/AO1010, PP/AO736, and PP/HP. It is worth noting that the mass fraction of antioxidant is maintained at approximately 3.2%.

2.2. Optimization Method

To eliminate internal stresses, the Geometry Optimization function in the Forcite module is employed to optimize the structure to minimize the energy of PP/antioxidant systems, with a maximum iteration step of 50,000. All models are dynamically refined for 500 ps, using the NVT ensemble at 300 K for initial equilibration and the NPT ensemble at 300 K for the second equilibration. Subsequently, an annealing process from 300 K to 800 K is implemented in NVT ensemble for 100 cycles, with each cycle consisting of 500 steps and a step size of 1 fs. Afterwards, the Dynamics function in the Forcite module is used to carry out volume relaxation, with the ensemble NPT, the temperature 300 K, and the relaxation time 100 ps. Ultimately, an amorphous PP/antioxidant model with appropriate density is obtained. The model is deemed physically representative when the density and energy of system maintains equilibrium in the MD relaxation treatment.

3. Calculation and Analysis of Thermal Properties

3.1. Glass Transition Temperature

3.1.1. Simulation Results

The macroscopic properties of polymers are strongly correlated with their microscopic structures [14]. As a critical parameter for characterizing the thermodynamic behavior, T_g corresponds to the lowest temperature at which molecular chains begin to move. When the temperature exceeds T_g, PP transitions from the glassy state to the high elastic state, accompanied by substantial changes in ther-

mal and electrical properties, especially near T_g.

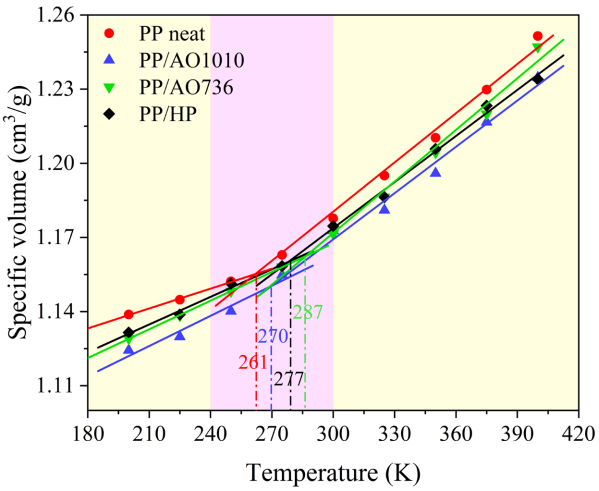

Figure 2. Glass transition temperature.

T_g is determined by analyzing the temperature-specific volume curves (see **Figure 2**). The simulated T_g of PP neat system is 261 K, which closely matches the experimentally reported range of 238 - 266 K [12], thereby verifying the accuracy of our simulation model. Obviously, introduction of three additives-AO1010, AO736, and HP-elevates T_g of PP to 270 K, 287 K, and 277 K, respectively, corresponding to the increases of 9 K, 26 K, and 16 K in comparison to PP neat.

3.1.2. Mechanism Analysis

On one hand, T_g is affected by the free volume fraction (FFV). According to free volume theory, the total volume of material is divided into two parts: free volume (V_F), representing the unoccupied space by molecular chains, and occupied volume (V_O), corresponding to the region actually occupied by molecular chains [9]. The distribution of V_F of neat PP in the temperature range of 200 - 400 K is illustrated in **Figure 3**, where the gray region signifies the surface area and the blue region denotes the V_F. In this section, FFV is introduced to compare the relative size of V_F. Its calculation formula is provided as follows [9]:

$$\mathrm{FFV} = \frac{V_F}{V_F + V_O} \times 100\% \tag{1}$$

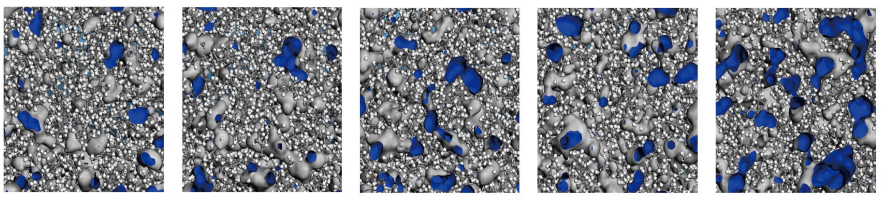

Figure 3. Free volume distribution of neat PP at different temperatures. (a) 200 K, (b) 250 K, (c) 300 K, (d) 350 K, (e) 400 K.

FFV of the four system is listed in Table 1. The composite systems exhibit lower FFV than that of PP neat system. This is attributed to enhanced intermolecular interactions induced by polar functional groups (e.g., hydroxyl groups). These interactions promote a more compact spatial arrangement of PP chains and restrict chains mobility, thereby elevating T_g of composite systems.

On the other hand, T_g is influenced by the molecular structure of antioxidants significantly. Specifically, the thiol group of AO736 captures free radicals and forms stable compounds, thereby terminating free radical chain reactions and enhancing antioxidant performance. In contrast, AO1010 has a large molecular structure that disrupts the continuity of hydrogen bond network, and HP contains a single phenol structure that limits hydrogen bond density. This is the reason why AO736 induces the most significant increase in T_g among the three composite systems.

Table 1. FFV of four systems at different temperatures.

Temperature (K) / System / FFV (%)	200	250	300	350	400
PP	9.15	10.86	13.41	14.59	18.76
PP/AO1010	8.76	10.69	11.84	13.94	17.62
PP/AO736	8.05	9.76	10.67	12.79	16.27
PP/HP	8.42	9.94	11.47	13.02	16.02

3.2. Thermal Conductivity

λ, a critical property governing heat transfer in materials, determines their heat dissipation capacity and thermal stability. Improving λ of PP can effectively suppresses the operating temperature rise rate and prevents thermal aging to extend its service life. λ of PP is calculated via the reverse nonequilibrium molecular dynamics (RNEMD) method [15]. In the simulation, the computational domain is partitioned into 40 equidistant slabs along the z-axis (see Figure 4, where $+\Delta E$ represents the energy transfer from hot to cold regions), and the terminal and central slabs are set as heat source and cold source, respectively. Through periodic momentum exchange between the lowest-energy particle in the heat sources and the highest-energy particle in the cold sources, the system attains equilibrium after a specific number of exchanges. This process can establish a steady-state heat flow under the nonequilibrium conditions, and ultimately the model will achieve a stable temperature gradient.

Figure 5 illustrates the simulated λ of four systems across the temperature span of 270 - 450 K. λ of PP neat system ranges from 0.103 to 0.139 W/(m·K). The simulation results are in good agreement with the experimental data reported in [16], therefore validating the reliability of our simulation model. All systems display a near-linear relationships between λ and temperature (T). At 300 K, λ of PP/AO1010, PP/AO736, and PP/HP systems increase by 10.9%, 17.6%, and 33.1%, respectively, when compared to PP neat. This is attributed to that antioxidants

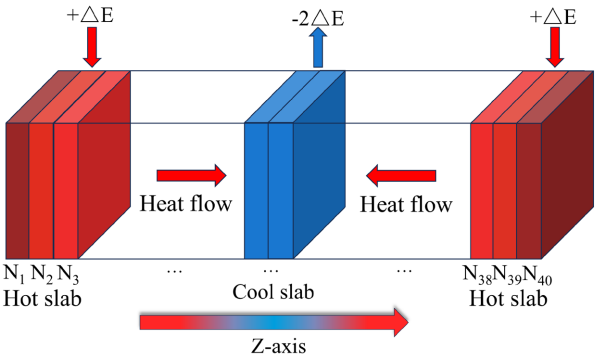

Figure 4. Schematic diagram of RNEMD method.

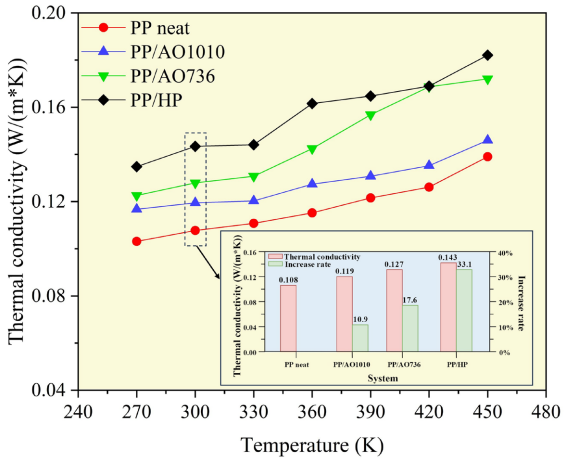

Figure 5. Thermal conductivity.

inhibit oxidation reactions, maintain the structure stability of PP molecules, and promote the formation of phonon transport pathways. In comparison with AO1010, AO736 and HP can further optimize the interfacial bonding between fillers and matrix through chemical interactions due to containing reactive functional groups; especially, HP shows the most superior λ enhancement due to its molecular characteristics, such as low molecular weight, high dispersibility, inducing heterogeneous nucleation in the PP matrix.

4. Calculation and Analysis of Electrical Properties

4.1. Relative Dielectric Constant

ε_r describes the dielectric behavior of insulation materials, and it can reflect their polarization characteristics under the external electric field [17].

$$\begin{cases} \varepsilon_r = 1 + \dfrac{1}{3Vk_BT\varepsilon_0}\left(\left\langle M^2\right\rangle - \left\langle M\right\rangle^2\right) \\ \left\langle M^2\right\rangle = \dfrac{1}{N}\sum_{i=1}^{N} M_i^2 \\ \left\langle M\right\rangle^2 = \left(\dfrac{1}{N}\sum_{i=1}^{N} M_i\right)^2 \end{cases} \tag{2}$$

where M represents the dipole moment of system at a time step, N denotes the total time step, the physical parameters V, T, k_B, and ε_0 are defined as system volume, thermodynamic temperature, Boltzmann constant, and vacuum dielectric constant, respectively.

The simulated ε_r is presented in **Figure 6**. ε_r of PP neat system is 2.341, exhibiting less than 5% deviation from the experimental values (2.2 - 2.5) reported in [18], thus validating the reliability of our simulation model. Moreover, it can be observed that composite systems show a decrease ε_r, moreover, PP/AO736 demonstrates the lowest ε_r (13.88% reduction versus PP neat). This is attributed to their molecular interaction mechanisms: (i) Multiple phenolic hydroxyl groups of AO1010 lead to interfacial polarization through charge accumulation. (ii) Aldehyde groups of HP can participate in neutralization reactions, but it still exhibits strong polarity. (iii) Thioether groups of AO736 exhibit great effects on scavenging radicals and hydrogen peroxide, resulting in a decrease in charge carrier density and suppression of space charge accumulation.

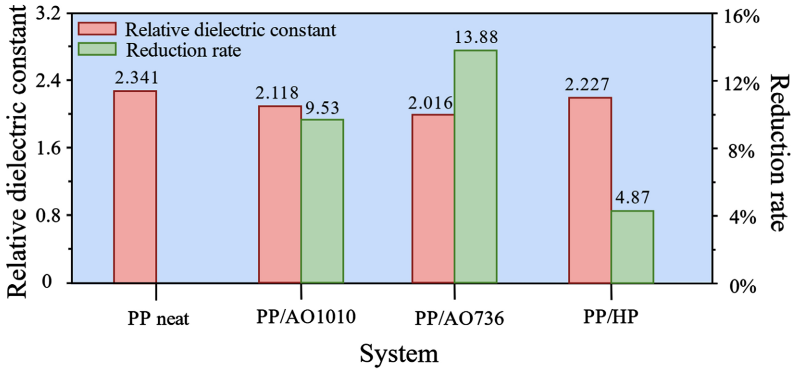

Figure 6. Relative dielectric constant.

4.2. Breakdown Strength

E_b refers to the threshold electric field at which a material loses capability of electrical insulation and undergoes electrical breakdown. Considering the inherent constraints of MD algorithms, it is difficult to accurately capture the cross-scale dynamic evolution. Therefore, in this section, E_b is calculated using the electro-mechanical breakdown theoretical framework [19].

4.2.1. Young's Modulus

Young's modulus (E) determines their processability and provides a quantitative measure of material rigidity and strength. It represents the intrinsic ability of a material to resist elastic deformation under stress [20]. We use the quasi-static constant strain method to calculate E across the temperature range of 180 - 480 K. This computational approach fundamentally relies on the constitutive relationship derived from continuum mechanics principles. The constitutive behavior of PP is governed by the framework of continuum mechanics, with its stress-strain relationship described by the generalized Hooke's law [21]

$$\begin{bmatrix}\sigma_1\\ \sigma_2\\ \sigma_3\\ \sigma_4\\ \sigma_5\\ \sigma_6\end{bmatrix}=\begin{bmatrix}C_{11} & C_{12} & C_{13} & C_{14} & C_{15} & C_{16}\\ C_{21} & C_{22} & C_{23} & C_{24} & C_{25} & C_{26}\\ C_{31} & C_{32} & C_{33} & C_{34} & C_{35} & C_{36}\\ C_{41} & C_{42} & C_{43} & C_{44} & C_{45} & C_{46}\\ C_{51} & C_{52} & C_{53} & C_{54} & C_{55} & C_{56}\\ C_{61} & C_{62} & C_{63} & C_{64} & C_{65} & C_{66}\end{bmatrix}\begin{bmatrix}\varepsilon_1\\ \varepsilon_2\\ \varepsilon_3\\ \varepsilon_4\\ \varepsilon_5\\ \varepsilon_6\end{bmatrix} \tag{3}$$

where C_{ij} denotes the elastic tensors, σ_i represents the engineering stress, and ε_j signifies the engineering strain. In the simulation, the amorphous PP can be approximated as an isotropic material [22], thus E can be given by

$$\begin{cases} E=\dfrac{\mu(3\lambda+2\mu)}{\lambda+\mu} \\ \lambda=\dfrac{1}{3}(C_{11}+C_{22}+C_{33})-\dfrac{2}{3}(C_{44}+C_{55}+C_{66}) \\ \mu=\dfrac{1}{3}(C_{44}+C_{55}+C_{66}) \end{cases} \tag{4}$$

where λ and μ are Lame constant. As illustrated in **Figure 7**, E of all systems exhibit a pronounced temperature dependence. When the temperature is below T_g, the restricted molecular chain results in V_F compression, promoting a packed arrangement of PP chains. As the temperature exceeds T_g, the activation of molecular chain motion drives V_F expansion, causing a rapid decrease in E. At 300 K, E of PP/AO1010, PP/AO736, and PP/HP systems are 2.70 GPa, 2.94 GPa, and 3.06 GPa, respectively, resulting in relative deviations of −4.93%, +3.52%, and +7.75% when compared to the PP neat system (2.84 GPa). AO1010 reduces the crystallinity of PP, thereby lowering its rigidity, whereas HP has the opposite effect. In contrast, AO736 improves rigidity via strengthening intermolecular interactions.

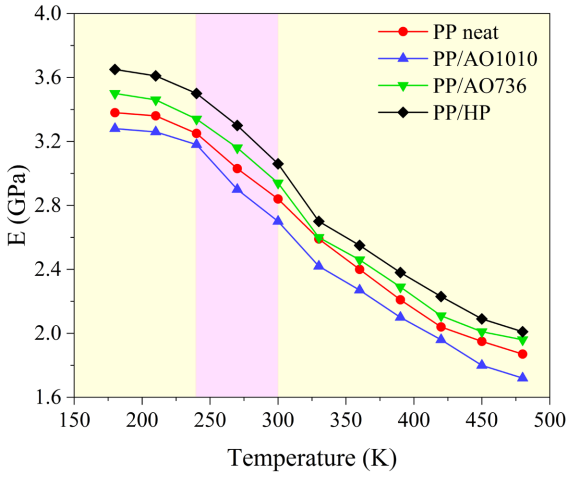

Figure 7. Young's modulus.

4.2.2. Calculation Results of Breakdown Strength

According to the electro-mechanical breakdown theory [19], E_b of PP can be approximately determined by

$$E_b = \left(\frac{E}{\varepsilon_0 \varepsilon_r} \right)^{\frac{1}{2}} \tag{5}$$

Figure 8 presents the calculated E_b at different temperatures. At 300K, E_b of PP neat is 397.1 kV/mm, with a relative error of less than 4.6% compared to the experimental value 416 kV/mm [8]. A universal decrease in E_b with rising temperature is observed in all systems, among which the PP/AO736 system exhibits the slowest rate of decline. Remarkably, E_b of four systems exhibit minimal variation at low temperatures (250 - 350 K). However, when the temperature exceeds 350 K, PP/AO736 system maintains superior electrical insulation property, achieving a 37.6% enhancement in E_b compared to that of neat PP at 400 K. Under elevated temperatures, the phenolic hydroxyl group in AO1010 is oxidized to a quinone structure, losing its free radical scavenging ability and thereby inducing thermal breakdown, and the aldehyde group in HP accelerates volatility, resulting in the decline of the neutralization efficiency of polar groups. By contrast, the thioether group in AO736 retains high reactivity, continuously decomposes hydroperoxides to suppress oxidation reactions, thus delaying the thermal breakdown.

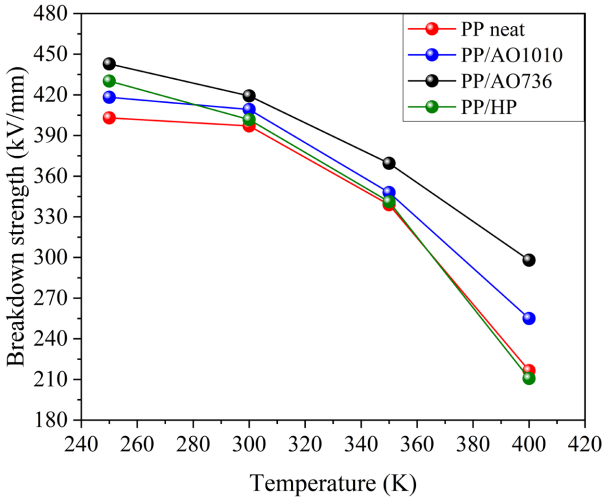

Figure 8. Breakdown strength.

5. Conclusions

- In terms of thermal properties, compared to PP neat system, the glass transition temperature of PP/AO1010, PP/AO736, and PP/HP composite systems is increased by 9 K, 26 K, and 16 K, respectively. Among them, AO736 exhibits the most notable improvement due to the strong interactions between its thioether groups and PP chains. At 300 K, thermal conductivity of these composite systems rises by 10.9%, 17.6%, and 33.1%, respectively. HP molecule with low molecular weight and high dispersibility manifests the greatest enhancement.
- Regarding electrical properties, the three composite systems display a decrease in relative dielectric constant by 9.53%, 13.88%, and 4.87%, respectively. Ad-

ditionally, at 400 K, the incorporation of AO736 enhances the breakdown strength of PP neat system by 37.6%. Mechanism analysis reveals that the three antioxidants can suppress the oxidation degradation of PP materials, reduce the accumulation of polar groups, and preserve the structural integrity of PP chains. However, only the thioether groups of AO736 retain high reactivity at high temperatures, thus demonstrating the best electrical insulation performance under such conditions.

- Antioxidant modification can achieve the synergistic optimization of the electrothermal performance of PP. AO736 significantly enhances the breakdown strength and glass transition temperature, while HP shows the most significant improvement in thermal conductivity. Future research will use both experimental and simulation methods for cross-verification, aiming to provide more comprehensive guidance for the design of high-performance PP insulating materials.

Acknowledgements Data

This work was jointly supported by the National Natural Science Foundation of China (No. 52307157) and Project supported by the Natural Science Foundation of Hunan Province, China (No. 2025JJ90178).

Availability Statement

Data will be made available on request.

Conflicts of Interest

The authors declare no conflicts of interest regarding the publication of this paper.

References

[1] Kim, D., Lee, S.H., Kwon, T.H., Kwon, I., Han, D.H., Park, H., *et al.* (2023) Study on High-Temperature and High-Voltage Insulation Characteristics of Polypropylene Blend with Highly Packed Elastomeric Domains for Power Cable Applications. *Polymer Testing*, **120**, Article ID: 107942. https://doi.org/10.1016/j.polymertesting.2023.107942

[2] Yang, K., Ren, Y., Wu, K., Li, J., Jing, Z., Zhang, Z., *et al.* (2022) Enhancing Electrical Properties of Impact Polypropylene Copolymer for Eco-Friendly Power Cable Insulation by Manipulating the Multiphase Structure through Molten-State Annealing. *Composites Science and Technology*, **223**, Article ID: 109422. https://doi.org/10.1016/j.compscitech.2022.109422

[3] Demirbas, Ö., Cetin, H., NAS, M.S., Calimli, M.H., Bayat, R. and Sen, F. (2025) Fabrication and Thermomechanical Property Investigations of Polypropylene/Silica and Polypropylene/Modified Silica Composite Films. *Next Materials*, **7**, Article ID: 100357. https://doi.org/10.1016/j.nxmate.2024.100357

[4] Guo, Y., Deng, J., Yu, H., Huang, Y. and He, B. (2024) Preparation and Properties of Self-Reinforced Polypropylene Composites Modified with β-Nucleating Agents. *Polymer*, **313**, Article ID: 127723. https://doi.org/10.1016/j.polymer.2024.127723

[5] Li, G., Chen, X., Guo, H., Liu, L., Li, S., Zhu, Y., *et al.* (2025) Insulation Properties of

Polypropylene and Silicone Rubber Modified by Barium Strontium Titanate and Interfacial Charge Accumulation Properties. *Composites Science and Technology*, **261**, Article ID: 111037. https://doi.org/10.1016/j.compscitech.2025.111037

[6] Yokoi, D., Takamura, M. and Takahashi, T. (2023) Mechanical Properties of Carbon Fiber/Polypropylene Composites Using Carboxylic-Acid-Modified Polypropylene without and with Oxazoline-Containing Polymer Coated on Carbon Fiber. *Composites Science and Technology*, **242**, Article ID: 110213. https://doi.org/10.1016/j.compscitech.2023.110213

[7] Chen, J., Du, K., Chen, X., Li, Y., Huang, J., Wu, Y., *et al*. (2019) Influence of Surface Microstructure on Bonding Strength of Modified Polypropylene/Aluminum Alloy Direct Adhesion. *Applied Surface Science*, **489**, 392-402. https://doi.org/10.1016/j.apsusc.2019.05.270

[8] Lee, O., Kim, D., Kim, H., Lee, S.H., Kwon, T., Kwon, I., *et al*. (2025) Improving the High-Voltage Insulation Properties of Polypropylene by Introducing Trace Addition of Polyvinylidene Fluoride: An Experimental and Simulation Study. *Composites Science and Technology*, **259**, Article ID: 110939. https://doi.org/10.1016/j.compscitech.2024.110939

[9] Guo, Y., Zhang, D., Zhang, X. and Wu, Y. (2023) Thermal Properties and Mechanical Behavior of Functionalized Carbon Nanotube-Filled Polypropylene Composites Using Molecular Dynamics Simulation. *Materials Today Communications*, **37**, Article ID: 107510. https://doi.org/10.1016/j.mtcomm.2023.107510

[10] Li, Y., Wang, Q. and Wang, S. (2019) A Review on Enhancement of Mechanical and Tribological Properties of Polymer Composites Reinforced by Carbon Nanotubes and Graphene Sheet: Molecular Dynamics Simulations. *Composites Part B*: *Engineering*, **160**, 348-361. https://doi.org/10.1016/j.compositesb.2018.12.026

[11] Zhu, L.W. and Du, B.X. (2018) Research Status on Electrical Tree of Polymer Insulation Materials in HVDC Cables. *Journal of Electrical Engineering*, **13**, 21-29. (In Chinese)

[12] Fu, Y.Z., Liu, Y.Q., Zhang, L.Y. and Lan, Y.H. (2009) Molecular Simulation of Glass Transition Temperatures of Polypropylene with Different Configurations. *Journal of Molecular Science*, **25**, 1-4. (In Chinese)

[13] Wang, D., Xuan, L., Han, G., Wong, A.H.H., Wang, Q. and Cheng, W. (2020) Preparation and Characterization of Foamed Wheat Straw Fiber/Polypropylene Composites Based on Modified Nano-TiO_2 Particles. *Composites Part A*: *Applied Science and Manufacturing*, **128**, Article ID: 105674. https://doi.org/10.1016/j.compositesa.2019.105674

[14] Zhou, Z., Yang, W., Yan, D. and Liu, H. (2013) Temperature Dependence of Polypropylene Configurations. *Macromolecular Theory and Simulations*, **23**, 76-83. https://doi.org/10.1002/mats.201300126

[15] Müller-Plathe, F. (1997) A Simple Nonequilibrium Molecular Dynamics Method for Calculating the Thermal Conductivity. *The Journal of Chemical Physics*, **106**, 6082-6085. https://doi.org/10.1063/1.473271

[16] Zhang, J., Zuo, J., Xu, S., Ju, A., Yuan, W., Zhang, J., *et al*. (2022) Enhancing the Electrical and Thermal Conductivity of Polypropylene Composites through the Addition of Sb-SnO_2/Coal Gasification Fine Slag Porous Microbead Powder. *Journal of Physics and Chemistry of Solids*, **169**, Article ID: 110843. https://doi.org/10.1016/j.jpcs.2022.110843

[17] Omelyan, I.P. (1996) On the Derivation of the Dipole Moment Fluctuation Formulas for Finite Systems. *Physics Letters A*, **212**, 279-284.

https://doi.org/10.1016/0375-9601(96)00061-8

[18] Adnan, M., Abdul-Malek, Z., Lau, K.Y. and Tahir, M. (2024) Tailored Dielectric Properties of Polypropylene Nanocomposites through Laboratory Synthesized Titania. *Materials Today Communications*, **41**, Article ID: 110919. https://doi.org/10.1016/j.mtcomm.2024.110919

[19] Lu, J., Zhu, B., Zhang, X. and Wang, X. (2019) Dielectric Strength Structure-Activity Relationship of BOPP Film for High Energy Density Pulse Capacitor. *IEEE Transactions on Plasma Science*, **47**, 4342-4349. https://doi.org/10.1109/tps.2019.2934762

[20] Granda, L.A., Espinach, F.X., Méndez, J.A., Tresserras, J., Delgado-Aguilar, M. and Mutjé, P. (2016) Semichemical Fibres of *Leucaena collinsii* Reinforced Polypropylene Composites: Young's Modulus Analysis and Fibre Diameter Effect on the Stiffness. *Composites Part B*: *Engineering*, **92**, 332-337. https://doi.org/10.1016/j.compositesb.2016.02.023

[21] Jindřich, N. and Ivan, H. (1981) Studies in Applied Mechanics. 3rd Edition, Elsevier, 41-55.

[22] Rajabi, K. and Hosseini-Hashemi, S. (2017) Application of the Generalized Hooke's Law for Viscoelastic Materials (GHVMs) in Nonlocal Free Damped Vibration Analysis of Viscoelastic Orthotropic Nanoplates. *International Journal of Mechanical Sciences*, **124**, 158-165. https://doi.org/10.1016/j.ijmecsci.2017.02.025